JACS
JOURNAL OF THE AMERICAN CHEMICAL SOCIETY
Article
pubs.acs.org/JACS

First Observation of a Kondo Resonance for a Stable Neutral Pure Organic Radical, 1,3,5-Triphenyl-6-oxoverdazyl, Adsorbed on the Au(111) Surface

Jie Liu,[†,‡] Hironari Isshiki,[†,‡] Keiichi Katoh,*[,‡,§] Takaumi Morita,[‡] Brian, K. Breedlove,[‡] Masahiro Yamashita,*[,‡,§] and Tadahiro Komeda*[,†,§]

[†]Institute of Multidisciplinary Research for Advanced Materials (IMRAM, Tagen), Tohoku University, 2-1-1, Katahira, Aoba-Ku, Sendai 980-0877, Japan

[‡]Department of Chemistry, Graduate School of Science, Tohoku University, Aramaki-Aza-Aoba, Aoba-Ku, Sendai 980-8578, Japan.

[§]JST, CREST, 4-1-8 Honcho, Kawaguchi, Saitama 332-0012, Japan

Supporting Information

ABSTRACT: We investigated spin states of stable neutral pure-organic radical molecules of 1,3,5-triphenyl-6-oxoverdazyl (TOV) and 1,3,5-triphenyl-6-thioxoverdazly (TTV) adsorbed on an Au(111) surface, which appears as a Kondo resonance because of spin-electron interaction. By using scanning tunneling spectroscopy (STS), a clear Kondo resonance was detected for the TOV molecule. However, no Kondo resonance was detected for TOV molecules with protrusions in the occupied state image and for TTV molecules. Spin-resolved DFT calculations showed that an unpaired π electron was delocalized over the adsorbed TOV molecule, which was the origin of the Kondo resonance. For the TOV molecules with protrusions, we proposed a model in which an additional H atom was attached to the TOV molecule. Calculations showed that, upon transfer of an electron to the verdazyl ring, the unpaired π electron disappeared, accounting for the absence of a Kondo resonance in the STS spectra. The absence of a Kondo resonance for the TTV molecule can be explained in a similar manner. In other words, electron transfer to the verdazyl ring occurs because of Au−S bond formation.

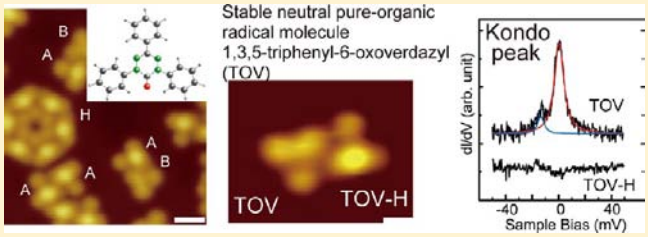

1. INTRODUCTION

Application of the freedom of spin and charge of an electron to the quantum process of information is called "spintronics".[1] Molecular spintronics is an emerging field that combines molecular electronics and spintronics.[2,3] Various types of spin blocks, including organic radicals, have been proposed.

The origin of the magnetism in the organic radicals is an unpaired π electron. These radical molecules are composed of light elements, such as C, N, O, and S. These elements have smaller spin−orbit coupling and hyperfine interactions, and provide longer spin coherent length than that of heavier elements used in inorganic electronic materials.[4] This is one of the reasons why organic molecules attract attentions as spin transport material. Moreover, by combining with photochromism and electrochromism,[5,6] the spin switching should be possible since there is a strong correlation between the structure and electronic properties. Applied researches were covered by a book by Hicks[7] and more recent review by Ratera.[8]

There have been intensive studies on stable organic radicals,[9,10] which include triarylmethyl (such as triphenylmethyl radical),[11] hydrazyl (such as DPPH = *N*,*N*-diphenyl-*N*′-picrylhydrazyl),[12] nitroxide (such as TEMPO = 2,2,6,6-tetramethylpiperidine-*N*-oxyl),[13] phenalenyl (such as TBPLY = 2,5,8-tritert-butylphenalenyl),[14] and thiazyl groups (such as 1,2,3,5-trithiadiazolyl radical).[15] In addition, the use of organic radicals in batteries,[16] oxidation catalysis,[17] living radical polymerization,[18] and spin labeling[19] have been studied.

The verdazyl radical of 1,3,5-triphenylverdazyl (TPV), which is a hydrazyl radical, was discovered in the 1960s by Kuhn and Trischmann (Scheme 1).[20] Several years after the first synthesis of TPV, Neugebauer synthesized 1,3,5-triphenyl-6-oxoverdazyl (TOV) and 1,3,5-triphenyl-6-thioxoverdazyl (TTV), which

Scheme 1

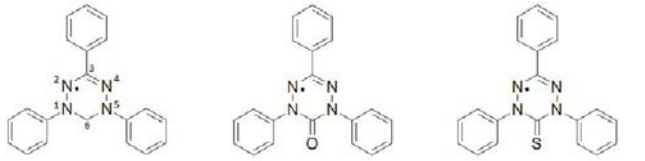

Received: April 20, 2012
Published: December 15, 2012

   dx.doi.org/10.1021/ja303510g | J. Am. Chem. Soc. 2013, 135, 651−658

contain a carbonyl group and a thiocarbonyl group at the C(6) position, respectively.[21]

The electronic structures of TOV and TTV have been examined by using X-ray crystallography, electronic absorption, EPR, ENDOR, and ^{2}H NMR spectroscopies,[21] and computational studies.[22] Although the crystal structure of TTV has not been obtained,[20,21] the amount of spin delocalization in TTV can be estimated by comparing it with that of 3-*t*-butyl-1,5-diphenyl-6-thioxoverdazyl.[20]

The spin delocalization can be seen in a series of 6-oxo- and 6-thioxoverdazyl molecules. In the verdazyl radical, the unpaired π electron, part of a 7π-electron system, is delocalized over the N(1)−N(2)−C(3)−N(4)−N(5) portion of the heterocycle. Thus, the singly occupied molecular orbital (SOMO) is mainly distributed over the four nitrogen atoms [(N(1)−N(2)−N(4)-N(5)] of the verdazyl ring.[22] C(6) is not formally conjugated because it is either saturated (sp^3), as it is in TPV or part of an exocyclic double bond, as it is in TOV and TTV.[21]

Switching of the magnetic character of verdazyl radicals been demonstrated using reversible one-electron oxidation (6π-cation) and one-electron reduction(8π-anion) processes.[23,24] The electrochemical properties are strongly influenced by the verdazyl structure and substituents, which makes this molecule a good building block for a construction of magnetic material. The magnetochemistry of verdazyl radical-based materials have been recently reviewed by Hicks[25] and Mukai.[26] Various verdazyl derivatives have been found to exhibit ferro-, weak ferro-, and antiferromagnetic intermolecular interactions between the $S = 1/2$ units in their crystals, which have exchange coupling energies ($\pm 2J/k_B$) on the order of a few to several tens of Kelvin.[7]

For actual applications, the formation of a film of the molecule is required. It has been demonstrated that a good quality films can be formed by a sublimation method. However, typical organic radicals cannot be sublimed in a vacuum due to their relatively low thermal stability. Therefore, the drop-cast methods have been used to form a film of the radical molecules.[27,28] Verdazyl radicals have a delocalized π-electron system compared with that of a nitroxide type radical, which makes the verdazyl radical molecules thermally stable (melting points are ∼200 °C).[21] Combined with the relatively small molecular weight (TOV = 327 g/mol and TTV = 343 g/mol), verdazyl radicals can be easily sublimated and deposited on substrates to form a film of good quality.

In this paper, we report the detection of a spin of a stable neutral pure-organic radical molecule adsorbed on a surface by observing a Kondo resonance, which is caused by the interaction between an isolated spin and a conduction electron,[29] using scanning tunneling spectroscopy (STS). Detection of a Kondo resonance using STS has been studied mainly for metal atoms adsorbed on a surface[30−35] or caged molecules.[36−40] Recently, it has been demonstrated that an unpaired π electron causes a Kondo resonance for double-decker phthalocyanato-Y(III) complexes (YPc_2)[41] and TCNQ molecules.[42] However, there are no reports of a Kondo resonance for pure organic radicals that are stable and neutral. In this study, we examined whether the spins of stable radicals, 1,3,5-triphenyl-6-oxoverdazyl (TOV) and 1,3,5-triphenyl-6-thioxoverdazly (TTV), adsorbed on the Au(111) surface could be detected as a Kondo resonance in STS spectra.

2. EXPERIMENTAL DETAILS AND CALCULATIONS

We synthesized TOV following a reported procedure.[43−49] We transferred the molecule to a substrate by using a sublimation method in an ultra high vacuum (UHV). Substrate cleaning, molecule deposition, and low-temperature STM observations were carried out in UHV chambers, whose details are described elsewhere.[50,51] The sample temperature was ∼4.7 K for the scanning tunneling microscopy (STM)/STS experiments described in this report. STS spectra were obtained by using a lock-in amplifier with a modulation voltage of 1 mV superimposed onto the tunneling bias voltage.

First-principle calculations were performed by using VASP code, employing a plane wave basis set and PAW potentials in order to describe the behavior of the valence electrons.[52,53] A generalized gradient Perdew−Burke−Ernzerhof (PBE) exchange-correlation potential[54] was used. Because of the absence of dispersion forces in the local and semilocal exchange-correlation approximations, the molecule-surface distance of a weak bonding case such as van der Waals interaction is overestimated, which is followed by an ambiguity of the charge transfer from the substrate to the molecule. Though many types of dispersion corrections methods have been developed including the one using semiempirical force-field,[55,56] the accuracy and the applicable target of each method is still not clear. Thus, they were not included in the current study. Nevertheless the calculation results for the adsorbed molecule can give a robust estimation for the understanding of STM images and spin behavior, if compared with the result calculated for the molecules placed in the vacuum. The structures were relaxed until the forces were smaller than 0.05 eV/Å. The gold surface was modeled as a 5-atom thick slab.

3. RESULTS AND DISCUSSION

The structures of TOV and TTV molecules placed in a vacuum were optimized by using the VASP calculation and are shown in Figure 1a. The TOV molecule is almost flat with the four six-member rings contained in a single plane. On the other hand, in the case of the TTV molecule, the S atom is bent out of the molecular plane. (See the Supporting Information) This is due to a larger radius of the S atom compared to that of the O atom, and the S atom was pushed away from the molecular plane to reduce the steric repulsion from the neighboring phenyls. For both molecules, the center ring has four N atoms, which is where the unpaired π electron is located.[47,57−61]

Figure 1b shows an STM image of TOV molecules adsorbed on a Au(111) surface. The clean Au(111) surface has a $(22 \times \sqrt{3})$ reconstruction, in which 23 atoms in a row along the close-packed direction occupy 22 bulk like positions. Some of the Au atoms were displaced from the usual fcc sites toward the hcp sites. In the process, some Au atoms are forced to occupy the high energy bridge sites, and, thus, were elevated above the surface. As a result, the surface had ridges between fcc and hcp valleys.[62−65] In enlarged image, chevron-shaped bends in the ridges were clearly observed.

The molecules adsorbed on both the fcc and hcp domains, but no molecules are found in the ridge region at this coverage. In addition to isolated and small clusters of molecules, we observed some circular molecule-assemblies at the elbow of the chevron which is known as an active site for adsorption of molecules.[62,65]

A magnified STM image is shown in Figure 1c. The molecule showed a triangle shape, which is consistent with the TOV molecule lying flat on the Au(111) surface. Dimers of TOV molecules, in which two TOV molecules were rotated 180° with respect to each other, were observed. In addition, we observed two different types of molecules: one had a protrusion in the center (type A), and the other did not (type B) in occupied state images. The dimers of both types of molecules

dx.doi.org/10.1021/ja303510g | J. Am. Chem. Soc. 2013, 135, 651−658

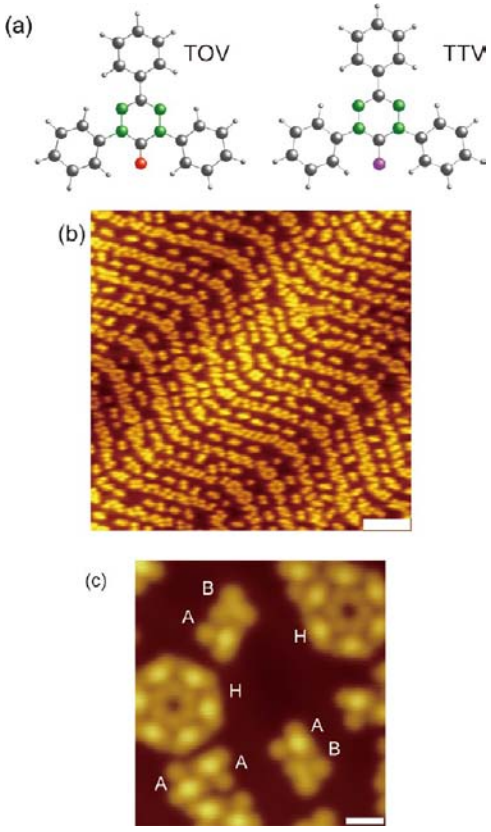

Figure 1. (a) Optimized model of a TOV and TTV molecules in a vacuum (gray, green, white, red, and purple balls represent C, N, H, O, and S, respectively). (b) Large area image of TOV molecules on Au(111). Scale bar = 200 Å, V_s = −0.8 V, I_t = 0.1 nA. (c) TOV dimers and hexamers. A, B, and H represent type A, type B TOV molecules and hexamers, respectively. Scale bar = 20 Å, V_s = −0.8 V, I_t = 0.1 nA.

are marked with A−B in the figure. Although we observed A−A dimers, we did not observe any B−B dimers. The circular assembly is a hexamer of the molecules. For the hexamer, which is marked H in the figure, protrusions were located at the perimeter of the six triangles, and no type B molecules were found in the hexamers.

High resolution images of the molecule, shown in Figure 2, were obtained to examine internal structures of the molecules. In the occupied state image of the type B molecule shown in Figure 2a, two of the three spots were slightly protruded than the other and there was a node in the middle of the triangle. In Figure 2b, an occupied state image of the A−B dimer is shown. The protrusion in the type A molecule was located in the lower part of the triangle and had a higher contrast than the three spots of the type B molecule did. The positions of the node and the protrusion of the type A molecules are shown in Figure 2c, where the protrusion is located on the symmetry line and next to a node

The change in the STM image with the bias polarity is shown for two pairs of A−A dimers in Figures 2d and e, which correspond to unoccupied and occupied state images, respectively. A homogeneous distribution of the image contrast was observed for the unoccupied state image, whereas the occupied state image showed a protruded spot in the middle. On the other hand, the occupied and unoccupied state images of type B molecules were basically the same.

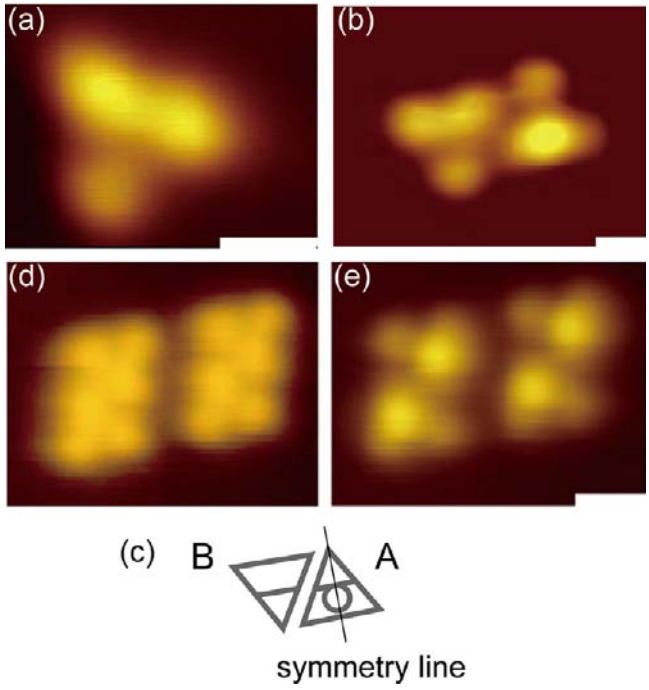

Figure 2. (a) Monomer and (b) dimer of TOV observed in occupied state. Scale bar = 10 Å, V_s = −0.8 V, I_t = 0.1 nA. (c) Sketch of dimer image. (d) Unoccupied state (V_s = 0.8 V) and (e) occupied state (V_s = −0.8 V) image of two pairs of A−A dimer. Scale bar =20 Å.

Next we examined the occupied state image of TTV molecules, which is shown in Figure 3. The shape of an

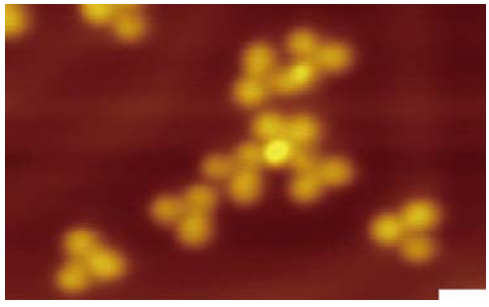

Figure 3. STM images of TTV on Au(111). Scale bar = 20 Å, V_s = −0.8 V, I_t = 0.1 nA.

individual TTV molecule is similar to that of the TOV molecule. However, in surfaces with similar coverages, the ratio of the type A molecules to the type B was much smaller for the TTV molecule than that for the TOV molecules. From Figure 3, the type B molecules, whose three spots were clearer than those of the TOV molecule, were more prevalent. Note that the protrusions in the molecules near the center are different from those of the type A molecules, since they are located at different sites. In addition, dimers and hexamers of the TTV molecules were scarcely observed.

STS spectra were acquired by using a lock-in amplifier. Figure 4a shows STS spectra around the Fermi level. Two spectra for the type A and B molecules in a single dimer are shown. The STS spectra obtained for the type B molecule clearly showed a sharp zero-bias peak (ZBP). We fitted the peak by using a Lorentzian function. The center of ZBP was determined to be at the Fermi level, and the full width half

dx.doi.org/10.1021/ja303510g | J. Am. Chem. Soc. 2013, 135, 651−658

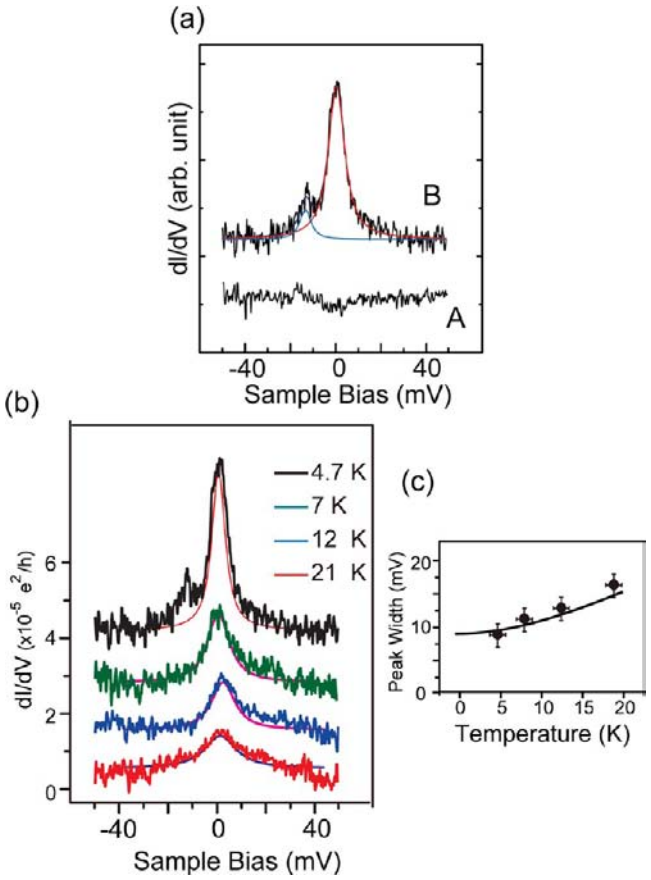

Figure 4. (a) STS spectra near the Fermi level observed of type A (plot A) and type B (plot B) TOV molecules. Background curves were subtracted. (b) Temperature dependence of the peaks measured in the region of 4.7−21 K. (c) Peak width changes vs temperature for the peak near the Fermi level. The solid curve indicates the fitted curve.

maxima (fwhm) of the dominant peak was ∼9 meV. When the STM tip was placed over the protrusion and the surrounding triangle part of a type A molecule, the STS spectra near the Fermi level was featureless (Figure 4a).

To prove that ZBP originates from Kondo resonance, we examined the change in the peak-width in relation to the sample temperature (see Figure 4b). The peaks were fitted using Lorentzian functions, and the fitted curves are plotted in the figure. FWHMs of the fitted curves are plotted in Figure 4c as solid circles. At elevated temperatures, it was difficult to observe a Kondo resonance due to thermal diffusion of the molecules owing to weak bonding between the TOV molecules and the Au(111) surface. Thus, a narrow temperature range was used.

Nagaoka et al. have introduced a function relating the changes in the Kondo-peak width to temperature ($\Gamma(T)$) using Fermi-liquid theory:[66] $\Gamma(T) = 2((\pi k_B T)^2 + 2(k_B T_K)^2)^{1/2}$, where k_B is the Boltzmann constant and T_K is the Kondo temperature. The observed data (solid circles) could be fitted using this formula, supporting the assignment of the ZBP as a Kondo resonance. The fitted curve is shown in Figure 4c as a solid line, and T_K was determined to be ∼37 K. The reported T_K values for adsorbed molecules vary widely: 150−550 K for CoPc on Au(111), which depend on the bonding configurations,[37] 357 and 589 K for FePc on Au(111) at two specific bonding sites,[67] 170 K for TBrPP-Co on Cu(111),[38] 26 K for TTF-TCNQ on Au(111),[42] and 30 K for $TbPc_2$ on Au(111).[41] The Kondo resonances in the last two cases originate solely from organic moieties.

The fact that the T_K value for the TOV radical (∼37 K) is similar to those for the $TbPc_2$ and TCNQ suggests that a common mechanism determines T_K for pure organic molecules. However, several things must be clarified to understand the T_K behavior. For example, it has been discussed that T_K is sensitive to the spin-substrate distance due to the change of hybridization between the molecule and the substrate.[37] Although the values of T_K for $TbPc_2$ and TOV are similar, the heights of the π orbitals responsible for the unpaired π electron (∼6 Å for the $TbPc_2$,[41] and ∼3.5 Å for TOV) are significantly different, as shown below. Further theoretical studies for Kondo resonance mechanism are required.

Site-dependent variation of the ZBP spectrum provides information about the nature of this peak. We examined the type B molecule in an A−B dimer, as shown in Figure 5a. The

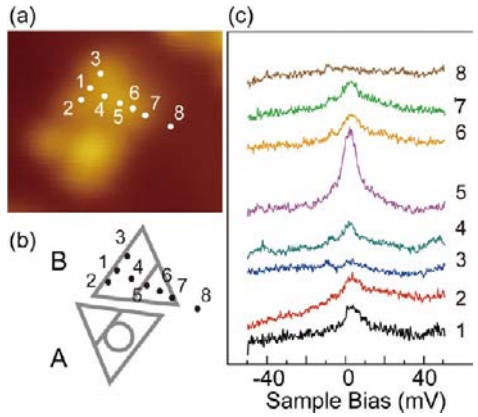

Figure 5. (a) STS detection positions on type B molecule in A−B dimer. (b) Illustration of a. (c) Changes of the Kondo resonance of the TOV molecule with the detection positions. Numbers for the positions in all panels are synchronized.

arrangement of the molecules is shown in Figure 5b. Changes in the ZBPs are shown in Figure 5c, for which the tip was positioned at the sites marked 1−8 in both Figures 5a and b. At position 8, which was over the bare Au(111) surface, the spectrum was featureless. At positions 1−7, Kondo resonances near the Fermi level were observed, and the strongest resonance was observed when the tip was over position 5.

In addition, we studied the ZBP for the TTV molecules with a surface coverage similar to that shown in Figure 3. However most of the spectra were featureless at the Fermi level. These results are clearly different from those for the TOV molecules.

Before comparing the experimental results with the simulations, we will discuss the effect of the electrons injected into the molecules. Photoinduced intramolecular spin alignment in complexes of anthracene-verdazyl radicals has previously been reported.[47,57−61] Photoexcitation occurs in the anthracene moiety, inducing an excited triplet state. Although the injected electron can cause such an excitation, in this case, the TOV molecules are isolated, meaning that intramolecular spin interaction is less likely to occur. In addition, the energy of the injected electron for the STS measurement is less than ∼50 meV, which is not strong enough to cause major electronic excitations.

We simulated STM images and calculated the spin-resolved density of states (DOS) using models, in which the TOV and

dx.doi.org/10.1021/ja303510g | J. Am. Chem. Soc. 2013, 135, 651−658

TTV molecules were either adsorbed on an Au(111) surface or suspended in a vacuum. An Au slab with five layers was used as the substrate. An optimized structure of a TOV molecule on an Au(111) surface shown in Figure 6(a). It was nearly flat like

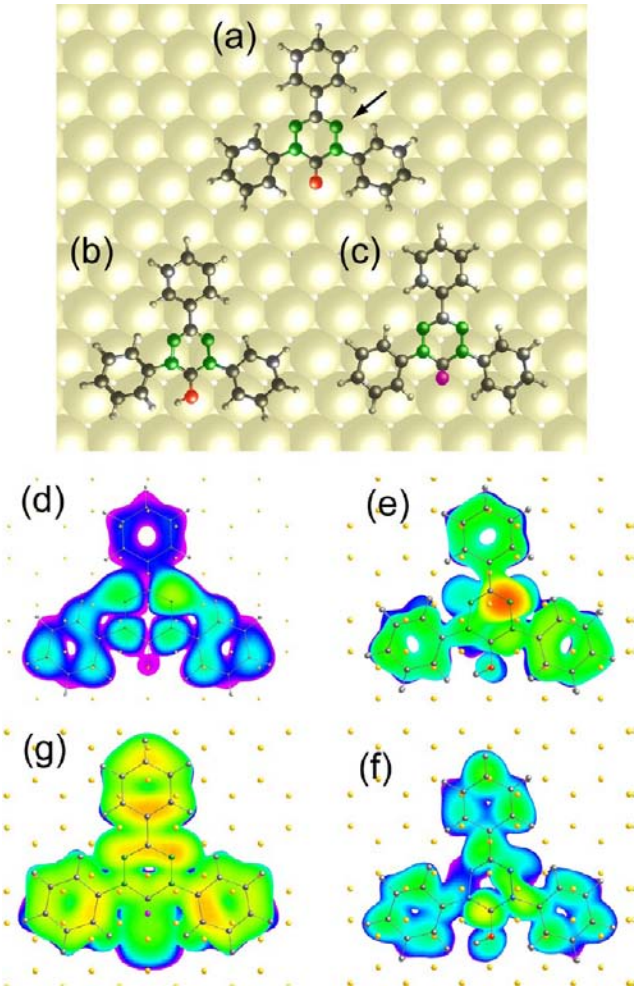

Figure 6. (a)−(c) Optimized adsorption structures for TOV (a), H-attached TOV (b), and TTV (c) molecules on Au(111) surface. (d)−(g) Simulated STM images of occupied-state TOV (d), occupied H-attached TOV (e), unoccupied H-attached TOV (f), and occupied TTV (g).

that in Figure 1a (see the Supporting Information). The plane was ∼3.5 Å higher than the topmost Au layer. This suggests that there is no direct bonding between O and Au atoms and that the height of the molecule is that of the molecule adsorbed on the surface via van der Waals interaction.[68]

A simulated STM image of the TOV molecule on an Au(111) surface is shown in Figure 6d, which was calculated for an energy range between 0 eV (Fermi level) and −0.5 eV in the occupied state. In this energy region, a dominant contribution from the SOMO state of the molecule is expected. As mentioned above, the SOMO level is the origin of the molecular spin, from which the Kondo resonance arises.

In the simulated image, most of protruded areas were located over the two N atoms of the upper part of the verdazyl ring. This coincides with the previous reports on the distribution of the SOMO level.[21,22] In addition, the lower two phenyl rings were more protruded than the top one was. The simulation reproduced the observed STM image of the type B molecule shown in Figure 2a, in which two of the three phenyl rings were more protruded than the others were.

The difference in the Kondo peak intensity at different tip positions shown in Figure 5 is related to the distribution of the SOMO level. In other words, position 5 in Figure 5, where the strongest Kondo resonance was observed, corresponds to the upper half of the verdazyl ring. Although there is a node along the vertical symmetry line of the molecule, the precision of our tip positioning was not good enough to pinpoint the node, and the SOMO state was detected on the upper N atoms.

Although other bonding configurations of the molecules were examined, we could not find a model that reproduced the protrusion of the type A molecule shown in Figure 2. However, we found that the images of the type A molecules could be reproduced by attaching an H atom to the oxygen atom of the TOV molecules. Figure 6b shows an optimized structure of the TOV-H molecule on an Au(111) surface (see the Supporting Information). Simulated STM images for the occupied and unoccupied states are shown in Figures 6e and 6f, respectively.

An intense protrusion was observed at one of the four N atoms in the occupied state in Figure 6e. This is due to transfer of an electron to the verdazyl ring with addition of an H atom. We believe that the asymmetric distribution of the molecular orbital is determined by the orientation of the H atom added on the O atom, which breaks the symmetry of both the electronic and physical structure. In the unoccupied state image (Figure 6f), on the other hand, the image contrast was rather uniformly distributed. The carbon atom next to O atom is slightly protruded, but the height difference is not significant and might not be detected in the STM image. Simulations of the occupied and unoccupied states reproduced the bias-polarity dependent images in Figure 2d and e.

The ratio of type-A molecules to the total TOV molecules was estimated to be ∼47% by counting the molecules in the STM image. To investigate the origin of the H atom, we acquired a mass spectrum of the TOV molecule before deposition (see the Supporting Information). Peaks for a TOV and for hydrogenated TOV (TOV-H) were observed. From the spectrum, we estimated that ∼25% of the TOV molecules were hydrogenated. In other words, some of the type-A molecules are the hydrogenated molecules before deposition. However, this does not fully account for the amount of the observed type-A molecules.

To investigate the possibility of hydrogen attachment in the UHV chamber, we exposed the TOV deposited surface to hydrogen atoms. We formed atomic hydrogen from molecular hydrogen with using a 1450 °C W filament placed 5 cm away from the sample surface. During this procedure, the UHV chamber was backfilled with 1×10^{-4} Pa H_2 for 600 s and the sample temperature was kept at RT.

As shown in the image in the Supporting Information, the portion of the type A molecule increased to be ∼90% of the total molecules. This indicates that the hydrogenation and formation of the type-A molecule also occurs in UHV condition. There are several possible origins for the H atom. For instance, the H atom could come directly from the vacuum or diffuse from the surface. Even under UHV conditions, H_2 remains. Metal surfaces as well as metal substrates can catalyze the dissociation of H_2, affording H atoms.

An optimized adsorption configuration of the TTV molecule on the Au(111) surface is shown in Figure 6c (See the Supporting Information). We should note that the S atom makes a chemical bond with the Au atom. The distance

dx.doi.org/10.1021/ja303510g | J. Am. Chem. Soc. 2013, 135, 651−658

between the S atom and the nearest neighbor Au atom was determined to be ~2.7 Å, which is in the range of the Au−S bond lengths calculated for alkanethiols with different alkane chain lengths on an Au(111) surface.[69] The stronger interaction between the molecule and the Au substrate enhances the exchange of charges between them. The S atom is located close to the 3-fold hollow site of the Au(111) surface.

The lack of type A molecules in the STM image and the chemical bond between S and Au atoms support the model, in which type A molecules of TOV are due to the addition of an H atom on the O atom of the TOV molecule. It is less likely that an additional H atom is attached to the TTV molecule once the Au−S bond is formed.

A simulated STM image for a TTV molecule in the occupied state is shown in Figure 6g, in which the height of the protrusion is distributed uniformly. The simulated image reproduced the observed image of TTV shown in Figure 3.

In Figure 7, we show partial density of states (PDOS) of the molecules discussed above determined from DFT calculations

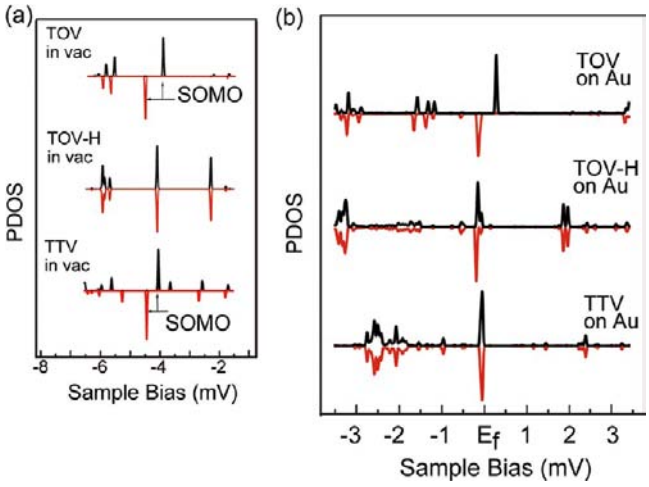

Figure 7. (a) Calculated spin-resolved partial density of state (PDOS) on the N atoms for the TOV, TOV-H, and TTV molecules placed in the vacuum. Red- and black-plots represent spin-up and -down components, respectively. (b) Same as a but the molecules were placed on the Au(111) surface.

on the N atom in the upper part of the verdazyl ring (marked by an arrow in Figure 6a). Figure 7a shows the PDOSs of a TOV molecule in a vacuum, the effect of the addition of an H atom, and a TTV molecule in a vacuum. The plot of the TOV molecule showed a clear split between the spin-up and down components. In the state marked "SOMO", only the spin-up component was occupied. This is consistent with the discussion of the radical TOV molecule above. Addition of an H atom caused the SOMO state to disappear, and no unpaired state was observed in the vacuum. This is due to a transfer of an additional electron to the verdazyl ring upon addition of the H atom, causing the electrons to pair. The TTV molecule shows a SOMO feature similar to that of the TOV molecule, which originates from the unpaired π electron.

The PDOSs for the three molecules adsorbed on the Au(111) surface were shown in Figure 7b. The SOMO state survived for the TOV molecule upon adsorption on the Au(111) surface. The disappearance of the SOMO state for TOV-H is same as that in Figure 7a.

In the case of TTV, the SOMO state disappeared after it was adsorbed on an Au(111) surface. As already mentioned, an Au−S bond forms upon adsorption, and thus, transfer of an additional electron to the verdazyl ring occurs through a similar pathway as that when an H atom adds to the TOV molecule. Finally, the SOMO state disappeared, and no Kondo resonance was observed in the STS spectrum, which is similar to the TOV case.

To understand the preferential formation of A−A and A−B dimers over that of B−B dimers for the TOV molecules, we calculated the distribution of the charge by integrating all of the valence bands of the TOV and TOV-H in a vacuum (see Figure 8). In the case of TOV-H, the charge density on the N atom

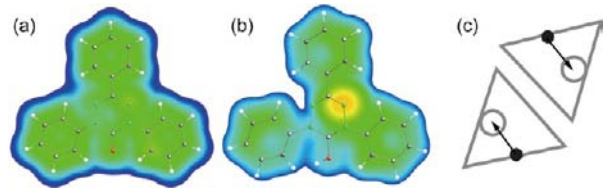

Figure 8. Distribution of the integrated charge of the valence bands of (a) TOV and (b) H-added TOV molecules in a vacuum. (c) Schematic of the protrusion (open circle) and O atom (solid circle) of the A−A dimer shown in Figure 2e. The arrow is the direction of the dipole.

was greater than that on the O atom, whereas in the case TOV, it was uniform, which is similar to the distribution of the SOMO level shown in Figure 6. This indicates that a dipole moment is formed between the N and O atoms of TOV-H.

It has been discussed that the dipole moment of organic molecules plays an important role in determining the ordered structure of organic films.[69] Figure 8c shows an illustration of an A-A dimer, in which the locations of the protrusions (N atoms) are marked by open circles. The positions of the O atoms are marked by solid circles, following the discussion in the previous section. The dipole moments of the two molecules align in opposite directions, which are indicated with the arrows in Figure 8c. The dipole−dipole interaction stabilizes the energy of the A−A dimer. In the A−B dimer, an induced-dipole interaction can occur. In other words, the A−A and A−B dimers of the TOV molecule preferentially form over B−B dimer. We think the hexamer of the type A molecules form for the same reason. However, further analysis of the dipole−dipole interaction is needed.

4. CONCLUSIONS

We investigated spin states of stable radical molecules of 1,3,5-triphenyl-6-oxoverdazyl (TOV) and 1,3,5-triphenyl-6-thioxo-verdazly (TTV) adsorbed on the Au(111) surface. In STS spectra, a clear Kondo resonance was detected for the TOV molecule. However for the TOV molecules with a protrusion in the occupied state image and for the TTV molecule, no Kondo resonance was detected. Spin-resolved DFT calculations showed that an unpaired π electron was delocalized over the adsorbed TOV molecule, which we believe to be the origin of the Kondo resonance. For the TOV molecule with a protrusion, we proposed a model in which an H atom attached to the TOV molecule (TOV-H). Calculation showed that, after an electron from the H atom was transferred to the verdazyl ring, the unpaired π electron disappeared, which accounts for the absence of a Kondo resonance in the STS spectra. The

dx.doi.org/10.1021/ja303510g | J. Am. Chem. Soc. 2013, 135, 651−658

disappearance of the Kondo peak for the TTV molecule was due to electron transfer to the verdazyl ring upon formation of an Au−S bond.

Our study showed that spin state of stable neutral pure organic radicals can be examined by the detection of the Kondo state using STM. By using this technique, submolecular spatial resolution and simultaneous characterization of both the adsorption configuration and spin state can be achieved. Moreover, we confirmed that the spin state of the molecule was sensitive to the bonding configuration. We believe this technique will become extensively used for investigating molecular magnetism.

■ ASSOCIATED CONTENT

Ⓢ Supporting Information

Molecular structures of TOV dimers. This material is available free of charge via the Internet at http://pubs.acs.org.

■ AUTHOR INFORMATION

Corresponding Author

komeda@tagen.tohoku.ac.jp; yamasita@agnus.chem.tohoku.ac.jp; kkatoh@m.tains.tohoku.ac.jp

Notes

The authors declare no competing financial interest.

■ ACKNOWLEDGMENTS

The authors are indebted to Dr. K. Suzuki for helpful discussions. T.K. acknowledges support from KAKENHI (22241026).

■ REFERENCES

(1) Wolf, S. A.; Awschalom, D. D.; Buhrman, R. A.; Daughton, J. M.; von Molnar, S.; Roukes, M. L.; Chtchelkanova, A. Y.; Treger, D. M. *Science* **2001**, *294*, 1488.

(2) Gatteschi, D.; Sessoli, R. *Angew. Chem., Int. Ed.* **2003**, *42*, 268.

(3) Bogani, L.; Wernsdorfer, W. *Nat. Mater.* **2008**, *7*, 179.

(4) Rocha, A. R.; Garcia-Suarez, V. M.; Bailey, S. W.; Lambert, C. J.; Ferrer, J.; Sanvito, S. *Nat. Mater.* **2005**, *4*, 335.

(5) Irie, M. *Chem. Rev.* **2000**, *100*, 1683.

(6) Yamase, T. *Chem. Rev.* **1998**, *98*, 307.

(7) Hicks, R. G. *Stable Radicals Fundamentals and Applied Aspects of Odd-Electron Compounds*; Wiley: Chichester, U.K., 2010.

(8) Ratera, I.; Veciana, J. *Chem. Soc. Rev.* **2012**, *41*, 303.

(9) Power, P. P. *Chem. Rev.* **2003**, *103*, 789.

(10) Lahti, P. M. *Magnetic Properties of Organic Materials*; Marcel Dekker, Inc: New York, 1999.

(11) Gomberg, M. *J. Am. Chem. Soc.* **1900**, *22*, 757.

(12) Alger, M. S. M. *Polymer Science Dictionary*; Springer: London, 1997; p 152.

(13) Likhtenshtein, G. I.; Yamauchi, J.; Nakatsuji, S., *Nitoroxides: Applications in Chemistry, Biomedicine, and Materials Science*. Wiley-VCH Verlag GmbH, Weinheim, Germany, 2008.

(14) Nakasuji, K.; Yamaguchi, M.; Murata, I.; Yamaguchi, K.; Fueno, T.; Ohyanishiguchi, H.; Sugano, T.; Kinoshita, M. *J. Am. Chem. Soc.* **1989**, *111*, 9265.

(15) Rawson, J. M.; Banister, A. J.; Lavender, I. *Adv. Heterocycl. Chem.* **1995**, *62*, 137.

(16) Nakahara, K.; Iwasa, S.; Satoh, M.; Morioka, Y.; Iriyama, J.; Suguro, M.; Hasegawa, E. *Chem. Phys. Lett.* **2002**, *359*, 351.

(17) Bobbitt, J. M.; Flores, M. C. L. *Heterocycles* **1988**, *27*, 509.

(18) Sciannamea, V.; Jerome, R.; Detrembleur, C. *Chem. Rev.* **2008**, *108*, 1104.

(19) Berliner, L. J., *Spin Labelling: Theory and Applications*. Academic Press: New York, 1979.

(20) Kuhn, R.; Trischmann, H. *Angew. Chem., Int. Ed.* **1963**, *2*, 155.

(21) Neugebauer, F. A.; Fischer, H.; Krieger, C. *J. Chem. Soc., Perkin Trans. 2* **1993**, 535.

(22) Berry, J. F.; Bill, E.; Bothe, E.; George, S. D.; Mienert, B.; Neese, F.; Wieghardt, K. *Science* **2006**, *312*, 1937.

(23) Gilroy, J. B.; McKinnon, S. D. J.; Kennepohl, P.; Zsombor, M. S.; Ferguson, M. J.; Thompson, L. K.; Hicks, R. G. *J. Org. Chem.* **2007**, *72*, 8062.

(24) Sporer, C.; Ratera, I.; Ruiz-Molina, D.; Zhao, Y.; Vidal-Gancedo, J.; Wurst, K.; Jaitner, P.; Clays, K.; Persoons, A.; Rovira, C.; Veciana, J. *Angew. Chem., Int. Ed.* **2004**, *43*, 5266.

(25) Koivisto, B. D.; Hicks, R. G. *Coord. Chem. Rev.* **2005**, *249*, 2612.

(26) Mukai, K. *Carbon-Based Magnetism*; Makarova, T.; Palacio, F., Eds.; Elsevier: Amsterdam, 2006; pp 75.

(27) Love, J. C.; Estroff, L. A.; Kriebel, J. K.; Nuzzo, R. G.; Whitesides, G. M. *Chem. Rev.* **2005**, *105*, 1103.

(28) Mas-Torrent, M.; Crivillers, N.; Mugnaini, V.; Ratera, I.; Rovira, C.; Veciana, J. *J. Mater. Chem.* **2009**, *19*, 1691.

(29) Kondo, J. *Phys. Rev.* **1968**, *169*, 437.

(30) Madhavan, V.; Chen, W.; Jamneala, T.; Crommie, M. F.; Wingreen, N. S. *Science* **1998**, *280*, 567.

(31) Li, J. T.; Schneider, W. D.; Berndt, R.; Delley, B. *Phys. Rev. Lett.* **1998**, *80*, 2893.

(32) Manoharan, H. C.; Lutz, C. P.; Eigler, D. M. *Nature* **2000**, *403*, 512.

(33) Knorr, N.; Schneider, M. A.; Diekhoer, L.; Wahl, P.; Kern, K. *Phys. Rev. Lett.* **2002**, *88*, No. 096804.

(34) Wahl, P.; Diekhoner, L.; Wittich, G.; Vitali, L.; Schneider, M. A.; Kern, K. *Phys. Rev. Lett.* **2005**, *95*, No. 166601.

(35) Neel, N.; Kroger, J.; Limot, L.; Palotas, K.; Hofer, W. A.; Berndt, R. *Phys. Rev. Lett.* **2007**, *98*, No. 016801.

(36) Zhao, A. D.; Li, Q. X.; Chen, L.; Xiang, H. J.; Wang, W. H.; Pan, S.; Wang, B.; Xiao, X. D.; Yang, J. L.; Hou, J. G.; Zhu, Q. S. *Science* **2005**, *309*, 1542.

(37) Zhao, A. D.; Hu, Z. P.; Wang, B.; Xiao, X. D.; Yang, J. L.; Hou, J. G. *J. Chem. Phys.* **2008**, *128*, 234705.

(38) Iancu, V.; Deshpande, A.; Hla, S. W. *Nano Lett.* **2006**, *6*, 820.

(39) Iancu, V.; Deshpande, A.; Hla, S. W. *Phys. Rev. Lett.* **2006**, 97.

(40) Perera, U. G. E.; Kulik, H. J.; Iancu, V.; da Silva, L.; Ulloa, S. E.; Marzari, N.; Hla, S. W. *Phys. Rev. Lett.* **2010**, 105.

(41) Komeda, T.; Isshiki, H.; Liu, J.; Zhang, Y.-F.; Lorente, N. s.; Katoh, K.; Breedlove, B. K.; Yamashita, M. *Nat. Commun.* **2011**, *2*, 217.

(42) Fernandez-Torrente, I.; Franke, K. J.; Pascual, J. I. *Phys. Rev. Lett.* **2008**, *101*, No. 217203.

(43) Mukai, K.; Konishi, K.; Nedachi, K.; Takeda, K. *J. Magn. Magn. Mater.* **1995**, *140*, 1449.

(44) Mukai, K.; Nuwa, M.; Suzuki, K.; Nagaoka, S.; Achiwa, N.; Jamali, J. B. *J. Phys. Chem. B* **1998**, *102*, 782.

(45) Fico, R. M.; Hay, M. F.; Reese, S.; Hammond, S.; Lambert, E.; Fox, M. A. *J. Org. Chem.* **1999**, *64*, 9386.

(46) Hicks, R. G.; Lemaire, M. T.; Ohrstrom, L.; Richardson, J. F.; Thompson, L. K.; Xu, Z. Q. *J. Am. Chem. Soc.* **2001**, *123*, 7154.

(47) Teki, Y.; Nakatsuji, M.; Miura, Y. *Mol. Phys.* **2002**, *100*, 1385.

(48) Train, C.; Norel, L.; Baumgarten, M. *Coord. Chem. Rev.* **2009**, *253*, 2342.

(49) Hou, Y. H.; Wang, H. K.; Li, Z.; Liu, Y. S.; Wan, X. J.; Xue, X. S.; Chen, Y. S.; Yu, A. *Tetrahedron Lett.* **2011**, *52*, 3670.

(50) Zhang, Y. F.; Isshiki, H.; Katoh, K.; Yoshida, Y.; Yamashita, M.; Miyasaka, H.; Breedlove, B. K.; Kajiwara, T.; Takaishi, S.; Komeda, T. *J. Phys. Chem. C* **2009**, *113*, 14407.

(51) Zhang, Y. F.; Isshiki, H.; Katoh, K.; Yoshida, Y.; Yamashita, M.; Miyasaka, H.; Breedlove, B. K.; Kajiwara, T.; Takaishi, S.; Komeda, T. *J. Phys. Chem. C* **2009**, *113*, 9826.

(52) Kresse, G.; Furthmuller, J. *Phys. Rev. B* **1996**, *54*, 11169.

(53) Kresse, G.; Joubert, D. *Phys. Rev. B* **1999**, *59*, 1758.

(54) Perdew, J. P.; Burke, K.; Ernzerhof, M. *Phys. Rev. Lett.* **1996**, *77*, 3865.

(55) Grimme, S.; Antony, J.; Ehrlich, S.; Krieg, H. *J. Chem. Phys.* **2010**, 132.

(56) Grimme, S.; Antony, J.; Schwabe, T.; Muck-Lichtenfeld, C. *Org. Biomol. Chem.* **2007**, *5*, 741.
(57) Teki, Y.; Kimura, M.; Narimatsu, S.; Ohara, K.; Mukai, K. *Bull. Chem. Soc. Jpn.* **2004**, *77*, 95.
(58) Teki, Y.; Nakatsuji, M.; Miura, Y. *Int. J. Mod. Phys. B* **2001**, *15*, 4029.
(59) Teki, Y.; Tamekuni, H.; Haruta, K.; Takeuchi, J.; Miura, Y. *J. Mater. Chem.* **2008**, *18*, 381.
(60) Toichi, T.; Teki, Y. *Polyhedron* **2005**, *24*, 2337.
(61) Mihara, N.; Teki, Y. *Inorg. Chim. Acta* **2008**, *361*, 3891.
(62) Barth, J. V.; Brune, H.; Ertl, G.; Behm, R. J. *Phys. Rev. B* **1990**, *42*, 9307.
(63) Wang, Y.; Hush, N. S.; Reimers, J. R. *Phys. Rev. B* **2007**, *75*, 233416.
(64) Chen, W.; Madhavan, V.; Jamneala, T.; Crommie, M. F. *Phys. Rev. Lett.* **1998**, *80*, 1469.
(65) Min, B.; Alemozafar, A.; Biener, M.; Biener, J.; Friend, C. *Top. Catal.* **2005**, *36*, 77.
(66) Nagaoka, K.; Jamneala, T.; Grobis, M.; Crommie, M. F. *Phys. Rev. Lett.* **2002**, *88*, No. 077205.
(67) Gao, L.; Ji, W.; Hu, Y. B.; Cheng, Z. H.; Deng, Z. T.; Liu, Q.; Jiang, N.; Lin, X.; Guo, W.; Du, S. X.; Hofer, W. A.; Xie, X. C.; Gao, H. J. *Phys. Rev. Lett.* **2007**, *99*, No. 106402.
(68) Toyoda, K.; Hamada, I.; Yanagisawa, S.; Morikawa, Y. *J. Nanosci. Nanotechnol.* **2012**, *11*, 2836.
(69) Franzen, S. *Chem. Phys. Lett.* **2003**, *381*, 315.